

# Refinability of splines from lattice Voronoi cells

Jörg Peters

October 31, 2021

## Abstract

Splines can be constructed by convolving the indicator function of the Voronoi cell of a lattice. This paper presents simple criteria that imply that only a small subset of such spline families can be refined: essentially the well-known box splines and tensor-product splines. Among the many non-refinable constructions are hex-splines and their generalization to non-Cartesian lattices. An example shows how non-refinable splines can exhibit increased approximation error upon refinement of the lattice.

## 1 Introduction

Univariate B-splines are defined by repeated convolution, starting with the indicator functions of a partition of the real line by knots (An indicator function takes on the value one on the interval but is zero otherwise). This construction implies local support and a number of desirable properties (see [dB78, dB87]) that have made B-splines the representation of choice in modeling and analysis. In particular, B-splines can be exactly represented as a linear combination of B-splines with a finer knot sequence. This refinability is a key ingredient of multi-resolution, adaptive and sparse representation of data.

By tensoring univariate B-splines, we can obtain on Cartesian grids in any dimension. For uniform knots, box-splines [dHR93] generalize this construction by allowing convolution directions other than the orthogonal ones of tensoring. This is not to say that box-spline convolution directions are arbitrary; to be practically useful, the directions need to be compatible with the lattice on which the spline is shifted, so that only a small number but sufficiently many lattice-shifts of the box-spline overlap at every point.

As a most prominent example in two variables, the three direction box-spline forms a function with hexagonal footprint. The function is called ‘hat function’ and consists of six linear function pieces over the constituent triangles. Shifts over an equilateral triangulation add up to 1. Convolution of this hat function with itself results in a twice continuously differentiable function of degree 4 and  $m$ -fold convolution yields a function of degree  $3m - 2$  with

smoothness  $C^{2m}$ . Since this progression skips odd orders of smoothness, van der Ville et al. [vBU<sup>+</sup>04] proposed to directly convolve the indicator function of the hexagon and build splines on the corresponding tessellation of the plane. They went on to show that the resulting hex-splines share a number of desirable properties familiar from box-splines. But the authors did not settle whether the splines were *refinable* [vdVU10], i.e. whether hex-splines of the given hexagonal tessellation  $T$  can be represented as linear combinations of hex-splines based on a finer-scale hexagonal tessellation, say  $\frac{1}{2}T$ . Refinability is important in practice since it guarantees monotonically decreasing approximation error as the scale of the tessellation refined. Moreover refinability is needed to locally adapt the space to features of higher frequency, a pre-requisite for multi-resolution analysis.

- This paper presents simple criteria on a lattice that need to hold in order for shift-invariant functions on that lattice to be represented as linear combinations of piecewise constant shift-invariant functions on the smaller-scaled copy of the lattice.

For example, the lattice must contain, for every of cell facet, the whole plane containing it. Therefore, requiring refinability, even of just the constant spline, strongly restricts allowable lattices.

- In contrast to tensor-product and box splines, we show that hex-splines and similar constructions can only be scaled, but not refined: scaled hex-spline spaces are not nested.
- A concrete example illustrates that non-refinable spaces can exhibit increased approximation error on a finer-scaled copy of the underlying tessellation (see Example 3).
- The analysis is extends to overcomplete spaces.

**Overview.** Section 2 reviews lattices, hex-splines and their generalizations. Section 3 exhibits two simple criteria for testing whether a lattice can support a refinable space of splines via convolution of indicator functions. Section 4 extends this investigation to overcomplete coverings by combining several families of indicator functions shifted by less than the lattice spacing. Section 5 illustrates the importance of refinability.

## 2 Splines from lattice Voronoi cells

A  $k$ -dimensional lattice is a discrete subgroup of full rank in a  $k$ -dimensional Euclidean vector space. A lattice may alternatively be viewed as a tessellation of space by identical cells. The Euclidean plane admits three highly symmetric tessellations into equilateral triangles, squares, or hexagons respectively. Convolution starting with the indicator function on any of these

polygons yields a hierarchy of spline functions of local support. The regular partition into squares gives rise to uniform tensor-product B-splines and the regular triangulation and its hexagonal dual to box splines. An interesting and natural complement, to convolve the indicator function  $H$  of the hexagon with itself, was developed and analyzed by van De Ville et al. [vBU<sup>+</sup>04]. This yields a family of splines, of smoothness  $n - 1$  supported on a local  $n + 1$ -neighborhood, that the authors named hex-splines. van De Ville et al. observed that hexagons are Voronoi cells of a lattice and that the cell can be split into three quadrilaterals using one of two choices of the central split. Thus  $H$  can be viewed as the union of three constant box splines [dHR93], an approach that was worked out more generally for the FCC lattice by [Kim08a] and in more generality in [ME10]. [vBU<sup>+</sup>04] compares tensor-product splines and hex-splines and presents a Fourier transform. The transform allows determining an  $L^2$  approximation order with emphasis on low frequencies, as a combination of projection into the hex-spline space and a quasi-interpolation error. [CvB05] derived quasi-interpolation formulas and showed promising results when applying hex-splines to reconstruction in image processing.

### 3 Refinability constraints for lattice Voronoi cells

Given a tessellation  $T$  of  $\mathbb{R}^k$ , we denote by  $\chi(T)$  the space of indicator functions over the cells of  $T$  and by  $\chi(T^1)$  the space of indicator functions on the smaller-scale copy  $T^1$  of  $T$ . The space  $\chi(T)$  is refinable if each indicator function in  $\chi(T)$  can be represented as linear combinations of functions in  $\chi(T^1)$ .

Testing whether a tessellation admits a refinable space of functions requires off hand solving for weights such that a linear combination of elements in  $\chi(T^1)$  with these weights reproduces each element in  $\chi(T)$ . Proposition 1 below provides a much simpler necessary condition that avoids such algebraic analysis. While we are interested in shift-invariant tessellations, Proposition 1 applies more generally.

**Proposition 1** *Let  $T$  be a tessellation of  $\mathbb{R}^k$  and  $T^1$  its smaller-scale copy. Then  $\chi(T)$  is refinable only if every tessellation facet of  $T$  is representable as a union of tessellation facets of  $T^1$ .*

**Proof** Since  $T^1$  is a tessellation, its cells do not overlap. Therefore, if a facet of a cell  $c$  in  $T$  is not a union of tessellation facets of  $T^1$  then a cell  $c'$  of  $T^1$  must cross this facet. Let  $H^1 \in \chi(T^1)$  be the indicator function of  $c'$  and  $H$  the indicator function of  $c$ . Then, in order to reproduce  $H$ ,  $H^1$  would have to take on both values 0 and 1. |||

Scaling of the tessellation transforms this criterion to a less local one.

**Proposition 2** For  $\chi(T)$  to be refinable, a tessellation  $T$  of  $\mathbb{R}^k$  must contain, for each facet, a whole plane of the same dimension parallel to it.

**Proof** Considering ever coarser tessellations, Proposition 1 implies that arbitrarily large extensions of each type of facet must be a union of tessellation facets of  $T$ . |||

The lattice structure implies that each such plane is replicated at all lattice points.

**Corollary 1** For  $\chi(T)$  to be refinable, if  $T$  is a lattice,  $T$  must contain, for every facet, the whole plane of the same dimension that contains it.

By inspection of the three regular tessellations of the plane, only the Cartesian grid and the uniform triangulation satisfy Corollary 1, but not the partition into hexagons.

**Corollary 2** Hex splines are not refinable.

We can generalize this observation by simplifying the inspection criterion.

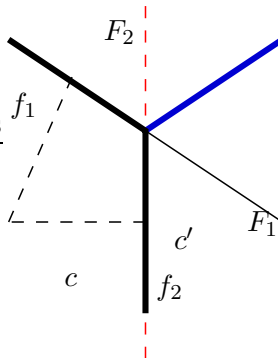


Figure 1: A pair of abutting facets, whose normals (dashed) have a strictly positive inner product, does not allow for refinability.

**Proposition 3** Consider a lattice  $T$  such that the reflection  $c'$  of a cell  $c$  across one of  $c$ 's facets is again a cell of  $T$ . If abutting cell facets of  $c$  meet with an obtuse angle then  $\chi(T)$  is not refinable.

**Proof** Let  $c$  be a cell of  $T$  with facets  $f_1$  and  $f_2$  that join with an obtuse angle (see Fig. 1). Let  $c'$  be the cell sharing  $f_2$ . By the reflection symmetry,  $c'$  also has an obtuse angle between  $f_2$  and the mirror image of  $f_1$  across the plane  $F_2$  through  $f_2$ . But on the side of  $c'$ ,  $F_1$  forms an acute angle with  $f_2$  and therefore intersects the interior of cell  $c'$ . Since cells can not be split,  $F_1$  cannot be part of  $T$  and the claim then follows from Corollary 1. |||

Proposition 3 allows us to quickly decide which of the (regular crystallographic) root lattices  $\mathcal{A}_n, \mathcal{A}_n^*, \mathcal{B}_n, \mathcal{D}_n, \mathcal{D}_n^*, \mathcal{E}_j, j = 6, 7, 8$  [CS98] are suitable for building splines by convolution of their Voronoi cells.

**Corollary 3** *Splines obtained by convolution of Voronoi cells of regular crystallographic root lattices are not refinable, except for the Cartesian grid and the bivariate lattice with triangular Voronoi cells.*

**Proof** We test whether the Voronoi cells of the root lattices contain a pair of faces that meet with an obtuse angle. We may assume that one cell center is at the origin and take the inner product of the position vectors of two adjacent nearest neighbors, as identified by their root system; if the product is strictly positive, the corresponding Voronoi faces meet with an obtuse angle.

The  $\mathcal{A}_n$  lattice is traditionally defined via an embedding in  $\mathbb{R}^{n+1}$ ,  $n > 1$ . Alternatively, Theorem 1 of [KP10] gives a convenient geometric construction in  $\mathbb{R}^n$  via the  $n \times n$  generator matrix  $\mathbf{A}_n := \mathbf{I}_n + \frac{c_n}{n} \mathbf{J}_n$ , where  $\mathbf{I}_n$  is the identity matrix,  $\mathbf{J}_n$  the  $n \times n$  matrix of ones and  $c_n := \frac{-1 + \sqrt{n+1}}{n}$ . Denoting the  $i$ th coordinate vector by  $\mathbf{e}_i$ , we choose  $\mathbf{e}_1$  and  $\mathbf{e}_1 + \mathbf{e}_2$  on the Cartesian grid, and map them via  $\mathbf{A}_n$  to the nearest  $\mathcal{A}_n$  neighbors of the origin. The inner product of the images of  $\mathbf{e}_1$  and  $\mathbf{e}_1 + \mathbf{e}_2$  is

$$\mathbf{A}_n \mathbf{e}_1 \cdot \mathbf{A}_n (\mathbf{e}_1 + \mathbf{e}_2) = \frac{n + 4c_n + c_n^2}{n} = \frac{2}{n} (n + \sqrt{n+1} - 1) > 0.$$

For the  $\mathcal{A}_n^*$  lattice, the computation is identical except that  $c_n := \frac{-1 + \frac{1}{\sqrt{n+1}}}{n}$ . The inner product is  $\frac{1}{n(n+1)} (n^2 - 2n - 2 + 2\sqrt{n+1}) > 0$ .

For the  $\mathcal{D}_n$  lattice, defined in  $n \geq 3$  dimensions, the generator matrix is  $\mathbf{D}_n := \begin{bmatrix} \mathbf{I}_{n-1} & -\mathbf{e}_{n-1} \\ -\mathbf{j}_{n-1}^t & -1 \end{bmatrix}$  (see e.g. Section 7 of [KP11]) and

$$\mathbf{D}_n \mathbf{e}_1 \cdot \mathbf{D}_n (\mathbf{e}_1 + \mathbf{e}_2) = 3 > 0.$$

Since  $\mathbf{D}_n^{-t}$  is the generator of  $\mathcal{D}_n^*$ , the inner product for  $\mathcal{D}_n^*$  is 2.

For  $\mathcal{B}_n$ , the Cartesian cube lattice has an inner product 0 identifying its spline constructions as potentially refinable (which indeed they are). On the other hand, splitting each the cube by adding a diagonal direction [Kim08b] yields the inner product  $\mathbf{e}_1 \cdot \mathbf{j} = 1$ .

For  $\mathcal{E}_6$ , we select the root vectors  $(1, 1, 0, 0, 0, 0)$  and  $(1, 1, 1, 1, 1, \sqrt{3})/2$  with inner product 1. For  $\mathcal{E}_7$ , we select the root vectors  $(1, 1, 0, 0, 0, 0, 0)$  and  $(1, 1, 1, 1, 1, 1, \sqrt{2})/2$  with inner product 1. For  $\mathcal{E}_8$ , we select the root vectors  $(1, 1, 0, 0, 0, 0, 0, 0)$  and  $\mathbf{j}_8/2$  with inner product 1.

Equilateral triangular Voronoi cells in  $\mathbb{R}^2$  yield the inner product  $-\frac{1}{2}$ .

|||

## 4 Overcomplete hex-spline spaces

Since the evaluation of hex-splines by convolving three families of box splines already leads to a large number of terms, it is reasonable to investigate whether redundant superposition make hex-splines refinable. To test whether we can build refinable frames, let  $\{T_j\}_{j=1..J}$  be a family of tessellations obtained by shifting  $T$  by less than the lattice spacing so that their union covers  $\mathbb{R}^k$   $J$ -fold. The next example makes this concrete for  $J = 3$ .

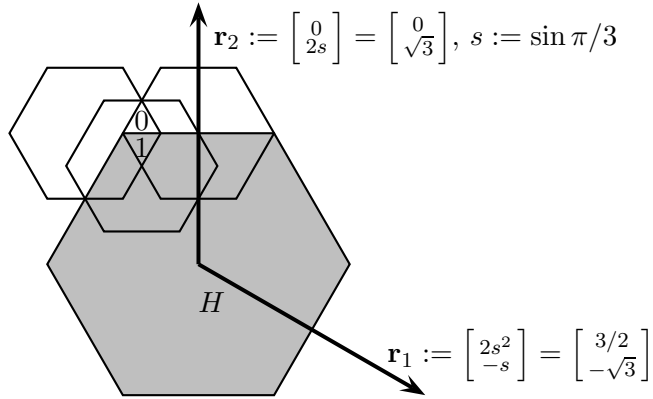


Figure 2: A lozenge-shaped pair of triangles (with markers 0 and 1) is in the common support of three half-scaled translated copies of the grey hexagon and not in the support of other half-scaled hexagons. Since the pair straddles the boundary of the hexagon, any linear combination of the three indicator functions needs to be both 1 and 0.

**Example 1** Denote by  $T_3$  a tessellation of the plane into unit-sized hexagons and by  $T_1$  and  $T_2$  its shifts by  $\frac{1}{2}\mathbf{r}_1$  and  $\frac{1}{2}\mathbf{r}_2$  (see Fig. 2). Let  $H(x)$  be the indicator function of the unit hexagon of  $T_3$  centered at the origin. Consider the three indicator functions of hexagons of the  $\frac{1}{2}$ -scaled tessellations shown in Fig. 2. Since the three hexagons supporting the three functions intersect in a pair of triangles, any linear combination of the functions has the same value on both triangles. But since the pair straddles the boundary of  $H(x)$  the value on one must be 0 and the value on the other 1 implying that the joint space is not refinable.

The example points to a simple extension of Corollary 1.

**Corollary 4** Consider a family  $\{T_j\}_{j=1..J}$  of tessellations each covering  $\mathbb{R}^k$ . Then the space  $\bigcup_{j=1..J} \chi(T_j)$  is refinable only if the tessellation obtained by intersecting  $\{T_j\}$  does not contain a cell straddling a cell facet of any coarser-scaled copy of any  $T_j$ .

The main argument concerning straddling cells applies to more general tessellations than shifts of a single tessellation  $T$ .

Extending the train of thought, the following Example 2 shows that families without straddling triangle pairs need not yield a refinable space of indicator functions either.

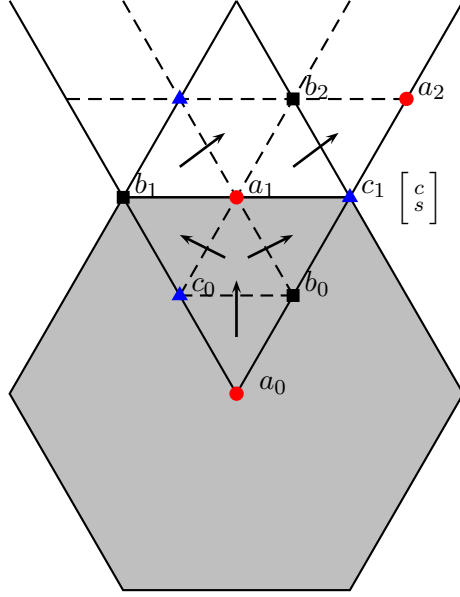


Figure 3: Propagation of values via neighboring triangles that share an edge. This yields the contradiction that  $a_0 + b_0 + c_0 = 1$  (center) and  $c_1 + b_2 + a_2 = 0$  (upper right) since the propagation implies  $a_i = a_0$ ,  $b_i = b_0$  and  $c_i = c_0$  for all  $i$ .

**Example 2** Consider shifts

$$H_2(x) := H\left(x - \begin{bmatrix} c \\ s \end{bmatrix}\right), \quad H_3(x) := H\left(x - \begin{bmatrix} -c \\ s \end{bmatrix}\right), \quad c := \cos \frac{\pi}{3}, \quad s := \sin \frac{\pi}{3}$$

of the indicator function  $H(x)$ . The three corresponding tessellations now intersect only in single triangles so that the scenario of Corollary 4 does not apply. However, an algebraic argument with a simple geometric interpretation proves lack of refinability.

We want to find scalar, real-valued coefficients  $a_i$ ,  $b_i$  and  $c_i$ ,  $i = (i_1, i_2) \in \mathbb{Z}^2$  such that the following refinement equation holds:

$$H(x) = \sum_{i=(i_1, i_2) \in \mathbb{Z}^2} a_i H(2x - \gamma_i) + b_i H_2(2x - \gamma_i) + c_i H_3(2x - \gamma_i),$$

$$\gamma_i := \frac{i_1}{2} \begin{bmatrix} c \\ s \end{bmatrix} + \frac{i_2}{2} \begin{bmatrix} -c \\ s \end{bmatrix}.$$

We associate the coefficients with the center of its support hexagon. Observe then that, when two triangles share an edge and  $H(x)$  has the same value  $v \in 0, 1$  on both triangles, then the coefficients at the two non-shared vertices must be equal. For example  $a_0 + b_0 + c_0 = v = a_1 + b_0 + c_0$  implies  $a_0 = a_1$ . As indicated by the arrows in Fig. 3, the coefficients are therefore propagated, separately inside and outside the support of  $H$ . This contradicts the refinement equation in that both  $a_0 + b_0 + c_0 = 1$  and  $a_2 + b_2 + c_1 = a_0 + b_0 + c_0 = 0$  must hold.

So even the two natural extensions to overcomplete spaces of shifted hexsplines do not afford refinability.

The propagation argument generalizes to face-sharing simplices in any dimension. And it generalizes from binary to  $m$ -ary refinement.

## 5 Importance of Refinability

Why do we care about refinability and nestedness of spaces? Approximation order is well-defined even for sequences of spaces that are not nested. For example, the elegant Fourier-based estimates of [vBU<sup>+</sup>04] show that hexsplines resulting from  $m$  convolutions have, for low frequencies, an  $L^2$  approximation order of  $m$ . But approximation order is concerned with asymptotic estimates. In practice one is more interested in predicting approximation error.

The following example shows why, for predicting the approximation error, nested spaces are highly desirable.

**Example 3** Let  $\mathcal{H}^i$  be the space of indicator functions over a regular tessellation by hexagons of diameter  $2^{-i}$  and such that, at each level of refinement, the origin is the center of one hexagon. Denote by  $H$  the indicator function in  $\mathcal{H}^0$  whose hexagon is centered at the origin. Let  $f$  be a  $C^1$  function obtained by smoothing out  $H$ , say by a degree 3 Hermite interpolant, over a distance of at most  $2\epsilon$  from the boundary of the hexagon.

Then the  $L^2$  approximation error to  $f$  from  $\mathcal{H}^0$  is approximately  $2\pi\epsilon$ , the integral over the smoothing region. However, since  $\mathcal{H}^1$  does not contain a linear combination that can replicate  $H$  (see Fig. 4b), the  $L^2$  approximation error to  $f$  from  $\mathcal{H}^1$  is approximately  $2\pi\frac{1}{2} \gg 2\pi\epsilon$ . That is the approximation error increases when refining the scale.

## 6 Conclusion

We identified simple necessary criteria for tessellations to admit a refinable space of (convolutions of) indicator functions. Lattices, in particular, must contain, for every facet, the whole hyperplane containing it. With

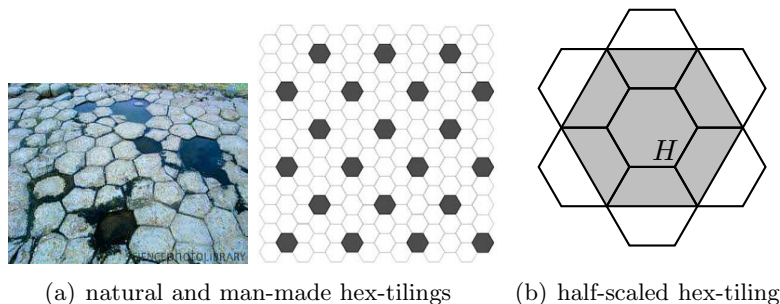


Figure 4: Examples for increased approximation error on a finer-scale tessellation. (a) Image credit to Simon Fraser and Fastfloors.com. (b) Non-nesting of the hex partition.

Corollary 3 we observed that the increased isotropy of the Voronoi cells of non-Cartesian root lattices prevents refinability. Increased isotropy of the Voronoi cells is however the main reason for considering non-Cartesian lattices in the first place: they have higher packing densities leading to more efficient sampling [PM62]. We observed that even overcomplete spaces obtained by natural superposition of shifted hexagonal tessellations fail to provide refinable spaces from convolution of indicator functions. Finally, and here we omit the details, of the semi-regular tessellations of the plane, only 3.6.3.6, the hex-tri-tessellation, satisfies the criteria of Proposition 1; and while its indicator functions are refinable, generalizing the construction by convolution fails to yield a family of higher-order splines sharing all good properties of box-splines.

In conclusion, if we want refinable classes of splines, remarkably few options exist apart of box splines and tensor-product B-splines. Conversely, it should be noted, that adjusting and combining the families of symmetric box-splines on crystallographic root lattices, exhibited and analyzed for example [KP11], does yield splines for any level of smoothness that obey the underlying symmetries.

**Acknowledgement** Zhangjin Huang kindly worked out the first proof of non-refinability for Example 1 and Example 2, two scenarios I posed. The current versions shorten his arguments.

## References

- [CS98] J. H. Conway and N. J. A. Sloane. *Sphere Packings, Lattices and Groups*. Springer-Verlag New York, Inc., New York, NY, USA, 3rd edition, 1998.

- [CvB05] L. Condat, D. van de Ville, and T. Blu. Hexagonal versus orthogonal lattices: A new comparison using approximation theory. In *ICIP*, pages III: 1116–1119, 2005.
- [dB78] C. de Boor. *A Practical Guide to Splines*. Springer, 1978.
- [dB87] C. de Boor. *B-form basics*, pages 131–148. SIAM, 1987.
- [dHR93] Carl de Boor, Klaus Höllig, and Sherman Riemenschneider. *Box splines*. Springer-Verlag New York, Inc., New York, NY, USA, 1993.
- [Kim08a] M. Kim. personal communication, e-mail to A Entezari and J Peters, April 09 2008.
- [Kim08b] Minho Kim. *Symmetric box-splines on root lattices*. PhD thesis, University of Florida, August 2008.
- [KP10] Minho Kim and Jörg Peters. Symmetric box-splines on the  $\mathcal{A}_n^*$  lattice. *Journal of Approximation Theory*, 162(9):1607–1630, September 2010.
- [KP11] M. Kim and J. Peters. Symmetric box-splines on root lattices. *Journal of Computational and Applied Mathematics*, 235(14):3972–3989, May 2011.
- [ME10] Mahsa Mirzargar and Alireza Entezari. Voronoi splines. *IEEE Transactions on Signal Processing*, 58(9), 2010.
- [PM62] Daniel P. Petersen and David Middleton. Sampling and reconstruction of wave-number-limited functions in  $N$ -dimensional Euclidean spaces. *Information and Control*, 5(4):279–323, December 1962.
- [vBU<sup>+</sup>04] D. van de Ville, T. Blu, M. Unser, W. Philips, I. Lemahieu, and R. van de Walle. Hex-splines: a novel spline family for hexagonal lattices. *IEEE Trans. Image Processing*, 13(6):758–772, June 2004.
- [vdVU10] D. van de Ville and M. Unser. personal communication, Banff, Nov 2010.